A High-Fidelity All-Textile UWB Antenna With Low Back Radiation for Off-Body WBAN Applications

Linda A. Yimdjo Poffelie, Ping Jack Soh, Sen Yan, and Guy A. E. Vandenbosch

***Abstract*—A novel all-textile UWB antenna with full-ground plane and high on-body fidelity is presented in this work. Due to the combined requirements of backward radiation reduction in WBANs and high-fidelity prerequisite for UWB pulse transmission/reception, a multilayered structure is implemented. The structure consists of two patches and a ground plane implemented on two layers of 2-mm-thick substrate. The full ground plane on the lower layer shields users against on-body radiation. Numerical and experimental evaluations both in free space and on human body prove the antenna operation within the FCC UWB bandwidth of 3.1–10.6 GHz. Its high-measured on-body system fidelity values of between 95% and 97% at a distance of 1 m show that the textile UWB antenna is suitable for body-worn UWB impulse radio communication.**

***Index Terms*—Conformal antennas, directional antennas, textile antennas, ultra wideband antennas, Wireless Body Area Network (WBAN).**

I. Introduction

The rapid development of wearable computing brought about the need to merge ultra-wideband (UWB) and textile technologies for practical antennas in body-centric wireless communications (BCWC) [1], [2]. BCWC systems such as wearable health monitoring systems potentially improve the quality of life by providing a low cost and real-time health status sensing and alerting in cases of emergencies, for instance. Antennas designed for wearable computing are, therefore, meant to operate in/on or close to the human body. UWB antennas are interesting candidates for low/medium data-rate wearable computing applications owing to their low power spectral densities (41.3 dBm/MHz) [3]. This is a very attractive feature for body-worn battery-operated devices. Besides their extremely low radiated power, UWB antennas designed for wearable computing need to be light weight, low profile, unobtrusive, and be shielded from the body to avoid safety risks. Apart from being capable of meeting these requirements, textile is the most suitable material to be integrated into human clothing as flexible antennas [4]–[9].

Most textile UWB antennas obtain their wide band behavior either by introducing slots on the radiating element/ground plane or by implementing partial rear ground planes [2], [4], [5], [10]. The main drawback of these topologies is that they radiate also in the backward direction, and this is undesirable for body worn communication since it introduces strong coupling to the human body. Recently, a new microstrip-based all-textile UWB antenna, implemented with a full rear ground plane, has been proposed to mitigate the aforementioned problem [6], [7].

Manuscript received March 9, 2015; revised November 23, 2015; accepted November 24, 2015. Date of publication December 17, 2015; date of current version February 01, 2016. This work was supported by Internal DOC Funds of the KU Leuven.

L. A. Yimdjo Poffelie, S. Yan, and G. A. E. Vandenbosch are with the ESAT-TELEMIC Research Division, Department of Electrical Engineering, KU Leuven, Leuven 3001, Belgium (e-mail: sen.yan@esat.kuleuven.be).

P. J. Soh is with the Advanced Communication Engineering (ACE) CoE, School of Computer and Communication Engineering, Universiti Malaysia Perlis, Arau 02600, Malaysia.

Color versions of one or more of the figures in this communication are available online at http://ieeexplore.ieee.org.

Digital Object Identifier 10.1109/TAP.2015.2510035

Another important issue that needs to be addressed in such body worn UWB textile antennas is their transmit/receive pulse characteristics. This is defined by the pulse fidelity factor (FF), which represents the amount of distortion introduced by the antenna on the transmitted/received pulse [11]. Fidelity values of up to 96% have been reported in [2] for all-textile UWB antennas. In order to achieve a satisfactory FF, narrow band square root raised cosine (SRRC) pulses were used to excite a planar monopole optimized using a modulated SRRC pulse [12], achieving an FF of 99.293% at 9.35 GHz. However, in all the above-mentioned antennas, the radiation pattern shows a bidirectional pattern due to the absence of a full ground plane.

In this communication, a full ground plane, all-textile UWB antenna with high-fidelity value is presented for off-body communications. The originality of this work lies in the fact that a minimal on-body irradiation is attained by the presence of the large reflector plane, while maintaining the wide bandwidth and high fidelities in free space and on body. This reflector plane results in the fact that the antenna shows a unidirectional radiation pattern and very low specific absorption rate (SAR) values, which is desirable for practical wearable antennas. Moreover, the additional parasitic patch enables the reflector plane to be placed close to the radiating structure, ensuring that the final antenna is wideband and low profile. To the best knowledge of the authors, the combination of these techniques to obtain a UWB bandwidth and a high-fidelity has yet to be reported for any antenna fully implemented using textiles.

This communication is organized as follows. Section II presents the description of the antenna design, materials, and its optimization process. Section III discusses numerical and measurement results, besides the implementation of the proposed antenna. Section IV discusses the results of the on-body performance measurements before this study is concluded in Section V.

II. Antenna Structure and Design

The initial design of the antenna is a grounded coplanar waveguide CPW-fed octagonally shaped UWB antenna (OSUA). An octagonal monopole is used in combination with beveling techniques to enhance the bandwidth [13]. This results in a 40.23×45.18 mm^2-sized patch and a wide bandwidth from 2 to 12 GHz. The drawback of this monopole structure is its bidirectional radiation pattern which is detrimental to the antenna performance when operating in proximity of a human body. To avoid the influence of the human body on the antenna, a full ground plane is directly added underneath the substrate layer as a reflector. In this way, a unidirectional radiation pattern is obtained but the impedance bandwidth is drastically reduced. This is remedied by using the concept of stacked patches. A parasitic patch is added beneath the radiating patch to enhance the bandwidth and maintain a relatively compact form factor and thickness. [14] After a very extensive simulation and optimization process, the final structure, optimized to balance the trade-off between bandwidth and size, is then obtained, as shown in Fig. 1(a).

The final design is a CPW-fed multistacked patch with a full reflector. It has the necessary bandwidth to cover UWB communications and a unidirectional radiation pattern extremely suited for wearable applications. Fig. 1(a) shows the optimized dimensions of the top and bottom patches. This design consists of two substrate layers and three metallic layers. The top metallic layer contains an octagonally shaped patch with an overall size of 33×30 mm^2 (width and length). This patch is fed using a grounded CPW feed line. A pair of steps is added onto both ground planes next to the feedline, which helps to enhance

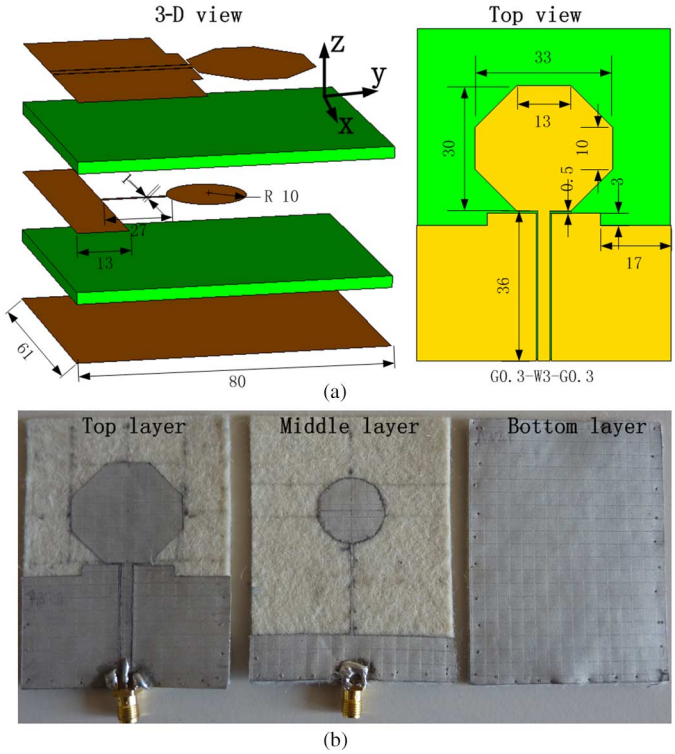

Fig. 1. Optimized dimensions in millimeter of the OSUA. (a) Stacked layer configuration and top patch (b) from left to right: fabricated top, middle and bottom metallic layers.

the bandwidth. The middle layer is a parasitic circular patch with 10-mm radius. This patch is connected by a thin strip to the ground. On the bottom layer of the antenna, a full metallic plane (reflector) is located.

The overall dimensions of the optimized antenna structure are $80 \times 61 \times 4.51$ mm^3, which is $0.849\ \lambda \times 0.647\ \lambda \times 0.048\ \lambda$ at the lowest operating frequency of 3.18 GHz. The relatively large antenna size is due to the relatively close placement of the full ground plane and parasitic, which simultaneously avoids on-body detuning and enlarges the operation bandwidth. The antenna performances are presented in the next section.

The prototype shown in Fig. 1(b) is fabricated using manual cutting tools and the process explained in [15]. The conductive components of the antenna (the patches, parasitic, and reflector) are built using ShieldIt conductive textile from LessEMF Inc. It has a thickness of 0.17 mm and an estimated conductivity of 1.18×10^5 S/m. Meanwhile, the substrate layers are formed using 2-mm-thick felt. Felt is a thermally isolating material with an estimated relative permittivity (ε_r) of 1.45 and a loss tangent (tan δ) of 0.044. A standard 50 Ω SMA connector model is used to feed the antenna via a grounded CPW feed line (top two layers). Note that the reflector in the bottom layer is nowhere connected to the connector. Galvanic connection from the SMA jack to the patches was performed by soldering at a maximum temperature of 250° C to avoid damaging the ShieldIt fabric. The structure is simulated using the time-domain solver within CST Microwave Studio.

III. Results and Discussion

As seen in Fig. 2, the agreement between simulated and measured reflection coefficient of the fabricated prototype in free space is satisfactory throughout the whole band from 3.18 GHz to more

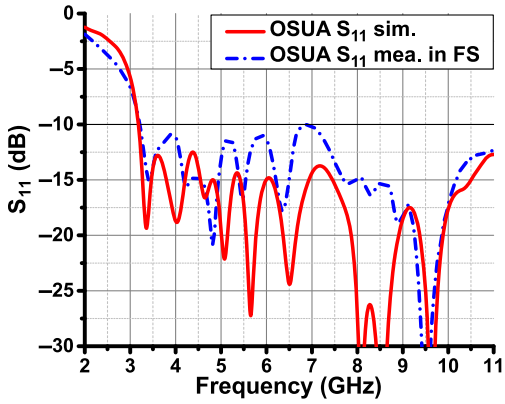

Fig. 2. Simulated and measured S_{11} in free space for the OSUA.

TABLE I
PROPERTIES OF HUMAN TISSUES FROM CST MATERIAL LIBRARY

Tissues	Density (kg/m^3)	$\varepsilon = \varepsilon' - j\varepsilon''$			Thickness (mm)
		3.5 GHz	5 GHz	10.5 GHz	
Skin	1100	37.2-j10.5	34.4-i13.1	30.8-j16.0	3
Fat	910	5.21-j0.85	4.82-j1.14	4.40-j1.29	7
Muscle	1041	52.1-j13.8	47.4-j19.4	41.2-j23.9	60

than 11 GHz. The little difference can be attributed to the fabrication tolerances (the antenna is totally made by hand) and numerical errors. [16]

Fig. 3 shows the antenna radiation patterns evaluated at 3.5, 7, and 10 GHz in the x–z and y–z planes. The measurements show that the main beam radiates away from the body, i.e., towards bore sight. This is already indicating that the antenna will have a low level of coupling with the human body, as will be shown in the following sections. The simulated gain is more that 5 dBi from 5 to 11 GHz, with a maximum gain of 7.2 dBi at 9 GHz. From 3 to 4.9 GHz, the gain varies from 4 to 5 dBi with a minimum of 1.1 dBi at 4 GHz.

IV. On-Body Evaluation

To validate the on-body performance of the OSUA, simulations as well as measurements were performed. SAR values at different frequencies were first calculated numerically using the three layer (skin–fat–muscle) human body model from [17]. The electrical properties of these body tissue layers are taken from the CST material library and are calculated from 3 to 11 GHz by using a third order interpolation model. The values at several frequencies are listed in Table I. This model has an overall area of 133×114 mm^2 and is placed 2 mm away from the antenna. The input power to the antenna in this work is set at 0.5 W (rms), and the SAR values were calculated based on the IEEE C95.1 standard, averaged over 10 g of biological tissue. The simulations show that the SAR values at the frequencies of 3, 6, and 10 GHz are all below the limit of 2 W/kg averaged over 10 g of tissue. The maximum SAR value is 1.21 W/kg at 3 GHz, whereas the lowest SAR value of 0.52 W/kg is found at 7 GHz.

The on-body S_{11} performance was evaluated on a female human volunteer weighing 66 kg and of height 1.59 m. The UWB antenna was placed on two different on-body locations, namely the chest and the arm, as shown in Fig. 4. The reflection coefficient (S_{11}) was measured in the frequency range 2–11 GHz in an anechoic chamber using a Hewlett Packard 8510C Vector Network Analyzer. During measurements, the UWB antenna was placed on either the chest or the arm and secured to the clothes using adhesive tape. The measured S_{11} with

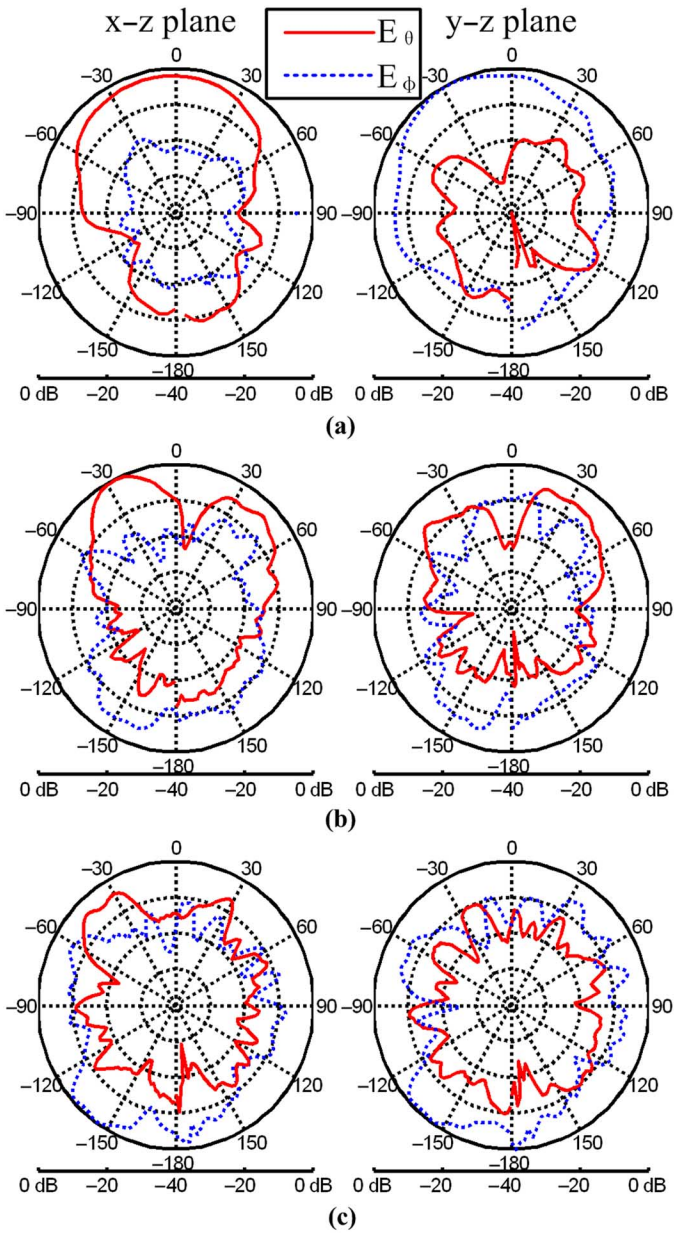

Fig. 3. Free space radiation patterns measured in an anechoic chamber in x–z and y–z planes at 3.5, 7, and 10 GHz.

Fig. 4. OSUA on-body measurement setup with the antenna placed on the chest and on the arm, respectively.

the OSUA placed on the chest and arm is shown in Fig. 5, indicating less than -10 dB throughout the entire UWB band and demonstrating the excellent on-body performance of the proposed antenna structure. The simulated radiation pattern does not change a lot in the upper half-space, which is the direction out off the body.

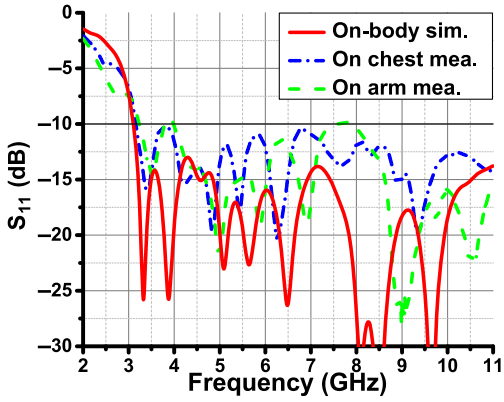

Fig. 5. Comparison of the on-body simulated and measured S_{11}.

Fig. 6. Free space fidelity (S_{12}) measurement setup in an anechoic chamber.

TABLE II
ON-BODY (OB) AND FREE SPACE (FS) COMPUTED SFF AT 0.5 AND 1 m

Rayleigh pulse type	Distance (m)	OB fidelity (%)	FS fidelity (%)
4th order, $\sigma = 76$ ps	0.5	99.3	99.4
	1.0	95.2	96.8
5th order, $\sigma = 91$ ps	0.5	99.4	99.4
	1.0	96.3	96.8
6th order, $\sigma = 106$ ps	0.5	99.6	99.6
	1.0	96.9	96.8

Frequency-domain transmission coefficient (S_{21}) measurements were performed using a pair of coaxial cables and two identical OSUAs facing each other at the distances of 0.5 and 1 m, both in free space and on body. The measurement setup for the free space S_{21} measurements is shown in Fig. 6. The measured S_{21} both in free space and on-body were used to evaluate the system FF as explained in [18] and [19]. The pulses used are a series of Rayleigh pulses with a pulse width of σ as shown in Table II. These pulses were chosen since it was shown in [11] that their spectra meet the FCC's emission limits. The mathematical formulas of this family of pulses both in the time and frequency domain are given below

$$v_n(t) = \frac{\mathrm{d}^n}{\mathrm{d}^n t}\left[e^{-\left(\frac{t-a}{\sigma}\right)^2}\right] \tag{1}$$

$$\widetilde{v}_n(\omega) = (j\omega)^n \sigma\sqrt{\pi} e^{-\left(\frac{\omega\sigma}{2}\right)^2} \tag{2}$$

where n represents the order of the Rayleigh pulse, a the center offset, and σ the time when the Gaussian pulse $v_0(\sigma) = e^{-1}$.

It was observed that a small misalignment between the two antennas in the measurement setup can occur, which could lead to some slight variations in the measured SFF. However, it was checked that if the angle difference between the two antennas is smaller than 30°, the

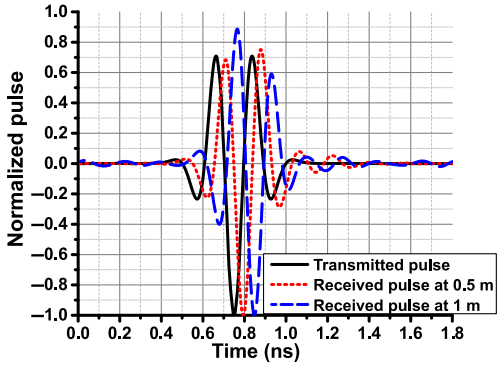

Fig. 7. On-body measured transmitted fifth-order Rayleigh pulse and calculated received pulses at 0.5 and 1 m.

TABLE III
COMPARISON WITH OTHER UWB ANTENNAS FROM LITERATURE

Ref. no	Antenna structure	Fully GD	Fidelity (%)	Radi ation pattern
[2]	UWB annular Slot antenna	No	96–99 (FS) 95–99 (OB)	Bidirectional
[10]	Antenna using LCP substrate	No	86–94 (FS)	Bidirectional
[9]	Antenna with truncated ground	No	Not evaluated	Bidirectional
[8]	Antenna using denim substrate	No	Not evaluated	Bidirectional
[4]	Planar monopole	No	Not evaluated	Bidirectional
[5]	Circular UWB antenna with centre hole	No	Not evaluated	Bidirectional
[6] and [7]	Textile UWB microstrip antenna	Yes	Maximum 87.9	Unidirectional
This work	Textile octagonal UWB antenna	Yes	96.9–99.6 (FS and OB)	Unidirectional

resulting SFF difference is negligible. The SFF is maintained above 0.9 and 0.8 for the distances of 0.5 and 1 m, respectively. Table II shows that the proposed antenna structure produces a minimal pulse distortion, comparable to its SFF in free space, and thus is suitable for off-body communication UWB applications. Theoretically, the FFs should not vary with distance. However, there are two reasons why there is a slight change in the measurements. 1) It is extremely difficult to ensure a perfect alignment during on-body measurements. A slight variation in fidelity is thus unavoidable. 2) At the distances measured, the receiving antenna is not in the far field of the "total radiator," i.e., transmitting antenna + body, or in other words, there is multipath introduced by the human body. Fig. 7 shows a fifth-order Rayleigh transmitted pulse. The received pulses are obtained by taking the convolution of the transmitted pulse and the Inverse Fourier Transform of the measured S_{12}.

Several other UWB antennas in the literature are compared in Table III. It can be seen that the design in this communication has the highest fidelity and more importantly, a unidirectional radiation pattern. That is the key feature of this wearable antenna.

V. CONCLUSION

A novel, UWB wearable textile antenna based on a combined stacked patch and parasitic coupling concept is proposed and discussed. The optimal top and bottom patches shapes led to a UWB characteristic with satisfactory simulated and measured bandwidths of more than 7.82 GHz, as required for UWB applications. The OSUA properties—high SFF value and maximum radiation in a direction normal to the radiator—are indicators that this antenna is suitable for wearable UWB impulse-radio in WBAN applications.

REFERENCES

[1] P. S. Hall and Y. Hao, *Antennas and Propagation for Body-Centric Wireless Communications*. Norwood, MA, USA: Artech House, 2006.
[2] M. Klemm and G. Troester, "Textile UWB antennas for wireless body area networks," *IEEE Trans. Antennas Propag.*, vol. 54, no. 11, pp. 3192–3197, Nov. 2006.
[3] Federal Communications Commission, "FCC report and order for Part 15 acceptance of ultra wideband (UWB) systems from 3.1-10.6 GHz," FCC, Washington DC, 2002.
[4] B. Sanz-Izquierdo, J. C. Batchelor, and M. I. Sobhy, "Compact UWB wearable button antenna," in *Proc. Antennas Propag. Conf.*, Loughborough, U.K., Apr. 2007, pp. 121–124.
[5] M. A. R. Osman, M. K. Abd Rahim, M. Azfar Abdullah, N. A. Samsuri, F. Zubir, and K. Kamardin, "Design, implementation and performance of ultra-wideband textile antenna," *Progr. Electromagn. Res. B*, vol. 27, pp. 307–325, 2011.
[6] P. B. Samal, P. J. Soh, and G. A. E. Vandenbosch, "UWB all-textile antenna with full ground plane for off-body WBAN communications," *IEEE Trans. Antennas Propag.*, vol. 62, no. 1, pp. 102–108, Jan. 2014.
[7] P. B. Samal, P. J. Soh, and G. A. E. Vandenbosch, "A systematic design procedure for microstrip-based unidirectional UWB antennas," *Progr. Electromagn. Res.*, vol. 143, pp. 105–130, 2013.
[8] M. E. Jalil, M. K. A. Rahim, M. A. Abdullah, and O. Ayop, "Compact CPW-fed ultra-wideband (UWB) antenna using denim textile material," in *Proc. Int. Symp. Antennas Propag.*, 2012, pp. 30–33.
[9] M. A. R. Osman, M. K. Abd Rahim, N. A. Samsuri, H. A. M. Salim, and M. F. Ali, "Embroidered fully textile wearable antenna for medical monitoring applications," *Progr. Electromagn. Res.*, vol. 117, pp. 321–337, 2011.
[10] Q. Abbasi, M. Ur-Rehman, X. Yang, A. Alomainy, K. Qaraqe, and E. Serpedin, "Ultrawideband band-notched flexible antenna for wearable applications," *IEEE Antennas Wireless Propag. Lett.*, vol. 12, pp. 1606–1609, Jan. 2014.
[11] Z. N. Chen, X. H. Wu, H. F. Li, N. Yang, and M. Y. W. Chia, "Considerations for source pulses and antennas in UWB radio systems," *IEEE Trans. Antennas Propagat.*, vol. 52, no. 7, pp. 1739–1748, Jul. 2004.
[12] A. Dumoulin, M. John, M. J. Ammann, and P. McEvoy, "Optimized monopole and dipole antennas for UWB asset tag location systems," *IEEE Trans. Antennas Propag.*, vol. 60, no. 6, pp. 2896–2904, Jun. 2012.
[13] M. Goudah and M. Y. M. Yousef, "Bandwidth enhancement techniques comparison for ultra wideband microstrip antennas for wireless application," *J. Theor. Appl. Inf. Technol.*, vol. 35, no. 2, pp. 184–193, Jan. 2012.
[14] C. A. Balanis, *Antenna Theory Analysis and Design*, 3rd ed. Hoboken, NJ, USA: Wiley, 2005.
[15] P. J. Soh, G. A. E. Vandenbosch, S. L. Ooi, and N. H. M. Rais, "Design of a broadband, all-textile slotted PIFA," *IEEE Trans. Antennas Propag.*, vol. 60, no. 1, pp. 379–384, Jan. 2012.
[16] G. A. E. Vandenbosch, "State-of-the-art in Antenna Software Benchmarking—'Are we there yet?'," *IEEE Antennas Propag. Mag.*, vol. 56, no. 4, pp. 300–308, Aug. 2014.
[17] J. Gemio, J. Parron, and J. Soler, "Human body effects on implantable antennas for ISM band applications: Models comparison and propagation losses study," *Progr. Electromagn. Res.*, vol. 110, pp. 437–452, Nov. 2010.
[18] G. Quintero, J.-F. Zurcher, and A. K. Skrivervik, "System fidelity factor: A new method for comparing UWB antennas," *IEEE Trans. Antennas Propag.*, vol. 59, no. 7, pp. 2502–2512, Jul. 2011.
[19] M. Sharma, A. Alomainy, and C. Parini, "Fidelity pattern analysis of a CPW-fed miniature UWB antenna using different excitation pulses," *IEEE Antennas Wireless Propag. Lett.*, vol. 14, pp. 494–498, Feb. 2015.